Effects of model resolution on ice shelf-ocean boundary layer

A. Malyarenko [1,2,3], S. Jendersie[2], N.J. Robinson[1], P.J. Langhorne[3], M.J.M. Williams[1] Corresponding author: alena.malyarenko@niwa.co.nz
[1] National Institute of Water and Atmospheric Research, Wellington, NZ; [2] National Modelling Hub, Antarctic Research Centre, Victoria University of Wellington, NZ; [3] Department of Physics, University of Otago, Dunedin, NZ.

Abstract

First, we investigate simulated ablation rates in a set of idealized ice shelf-ocean experiments with eleven different turbulent transfer coefficients (Γ_T and Γ_S) and five flux balance formulations. These pre-existing formulations were developed from observations, laboratory experiments, small-scale modelling and theoretical study of the ice-ocean boundary. In the present idealised numerical study, the mean ablation rate in warm cavity scenarios varies between 2.1 and 4.7 m year^{-1}, and in cold cavity scenarios between 0.03 and 0.17 m year^{-1}. The range of uncertainty in ablation rate is 0.07 m year^{-1} in cold cavity experiments and 1.43 m year^{-1} in warm cavity experiments.

Next, we compare effects of mixing strategies in the boundary layer. Γ_T and Γ_S not only directly determine the ablation rate, but have effects on fresh water distribution in the ocean boundary layer. High $\Gamma_{T/S}$ values develop deep mixed layers, while low $\Gamma_{T/S}$ values stratify the top ocean grid cells. Thus the ocean boundary layer structure directly depends on vertical resolution in the ocean model and how well the mixing scheme can handle the stratification effects. Without changes in vertical resolution, here we test counter effects of meltwater production, tidal mixing, ice shelf basal roughness and mixing schemes.

Model description

We have used the Met-ROMS (Naughten et al., 2018), which consists of the Regional Ocean Modelling System (ROMS v.3.7, Shchepetkin and McWilliams, 2005) coupled to the Ice Shelf model (Galton-Fenzi et al., 2012; Naughten et al., 2017). The model domain (ISOMIP domain 2, Asay-Davis et al., 2016; Hunter, 2006, based on Grosfeld et al., 1997), has 24 vertical levels; mixing, diffusion and advection schemes, and its initial and boundary conditions are identical to Gwyther et al. (2015, 2016). For the cold cavity scenario, the ocean surface is restored towards potential temperature -1.9°C and salinity 34.5. For the warm cavity scenario, the ocean surface is relaxed towards +0.5°C and 34.6 (Gwyther et al. 2015, 2016). The lateral boundaries are closed. Simulations were run for 30 years for the first part of the project, and the time-average of the last year is used in this analysis.

Name	Drag Coefficient: Low (Cd=0.0005)	Drag Coefficient: Control (Cd=0.003)	Drag Coefficient: High (Cd=0.1)	Turbulent transfer coefficient, Velocity-dependent, Variable: Version of Kader and Yaglom (1972) from Jenkins (1991)	Variable: Kader and Yaglom (1972), (eq. 30)	Variable: Yaglom and Kader (1974), (eq. 22) h=0.01	Variable: Kader and Yaglom (1977), (eq.14); h=0.01	Variable: McPhee et al. (1987) as in Schmidt et al. (2004), ROMS 3.3	Variable: McPhee et al., (1987) Stability parameter=1	Constant, Value: McPhee (2016), Section 5.3.9	Constant, Value: Kimura et al., (2016) Sec. 5.1	Constant, R, Ablation Value: 35	Constant, R, Ablation Value: 50	Constant, R, Ablation Value: 90	Constant, R: Freezing value = 1	Velocity-independent: Hellmer and Olbers (1989)	Flux Balance: Holland and Jenkins (1999): Only ablation case (eq. 31)	Only freezing case (eq. 31)	No advection case (eq. 21); & Hellmer and Olbers (1989)	Ablation – (eq. 21) Freezing – freezing case (eq. 31)	Ablation – ablation case (eq. 31) Freezing – (eq. 21)	Constant vertical advection case (eq. 31)
Control_HD			✓					✓														✓
Control		✓						✓														✓
Control_LD	✓							✓														✓
Balance_1		✓						✓												✓		
Balance_2		✓						✓									✓					
Balance_3		✓						✓											✓			
Balance_4		✓						✓										✓				
Balance_5		✓						✓													✓	
Gamma_1		✓		✓																		✓
Gamma_2		✓			✓																	✓
Gamma_3		✓				✓																✓
Gamma_4		✓					✓															✓
Gamma_5		✓							✓													✓
Gamma_6		✓								✓		✓										✓
Gamma_7		✓								✓			✓									✓
Gamma_8		✓								✓				✓								✓
Gamma_9		✓								✓		✓			✓							✓
Gamma_10		✓									✓											✓
Gamma_11		✓														✓						✓

Table 1. Experiments description (part 1 of the project). The chosen parameterization is marked with ticks.

The experiments are grouped as follows:

- The first set of experiments replicate experiments from Gwyther et al. (2015) with highest (Control_HD), lowest (Control_LD) and "commonly-used" (Control) values of the drag coefficient C_d.
- The second set of experiments (Gamma) covers $\Gamma_{T/S}$ expressions gathered from a range of studies that use varying assumptions of turbulence and stratification (the exact formulations of $\Gamma_{T/S}$ are provided in Table S1).
- In the third set of experiments (Balance) we apply various expressions for heat flux through ice shelf (Q_T^{ice}) combining Holland and Jenkins (1999) formulations with additional options available in Met-ROMS.

$\Gamma_{T/S}$ parameterisation effects

All experiments follow the general principle that large values of $\Gamma_{T/S}$ represent high ablation rates (Fig.1) and low gradient of temperature and salinity in the boundary layer. In general, higher ablation is associated with fresher and colder meltwater. Low mixing of the boundary layer, associated with low $\Gamma_{T/S}$, dampens both the heat flux from the ocean towards the interface (i.e. lowers ablation rates) and the salt flux from the interface towards the ocean (i.e. traps meltwater close to the interface causing strong stratification). Simulations show that the resulting area-averaged ΔT ranges from -0.13°C (Control_LD) to -0.02°C (Control_HD) for cold cavity conditions; and from -0.80°C (Control_LD) to -0.15°C (Gamma_3) for warm cavity conditions. ΔS ranges from -2.84 (Gamma_8) to -0.27 (Control_HD) for cold cavity conditions; and from -10.38 (Gamma_8) to -0.67 (Gamma_3) for warm cavity conditions. Experiments with lowest $\Gamma_{T/S}$ resulted from parameterisations with high values of R, similar to those observed under sea ice ($R=50$ within the range of recommended values of Notz et al. 2003) and modeled for balances calculated at the interface ($R=90$, Keitzl et al., 2016b).

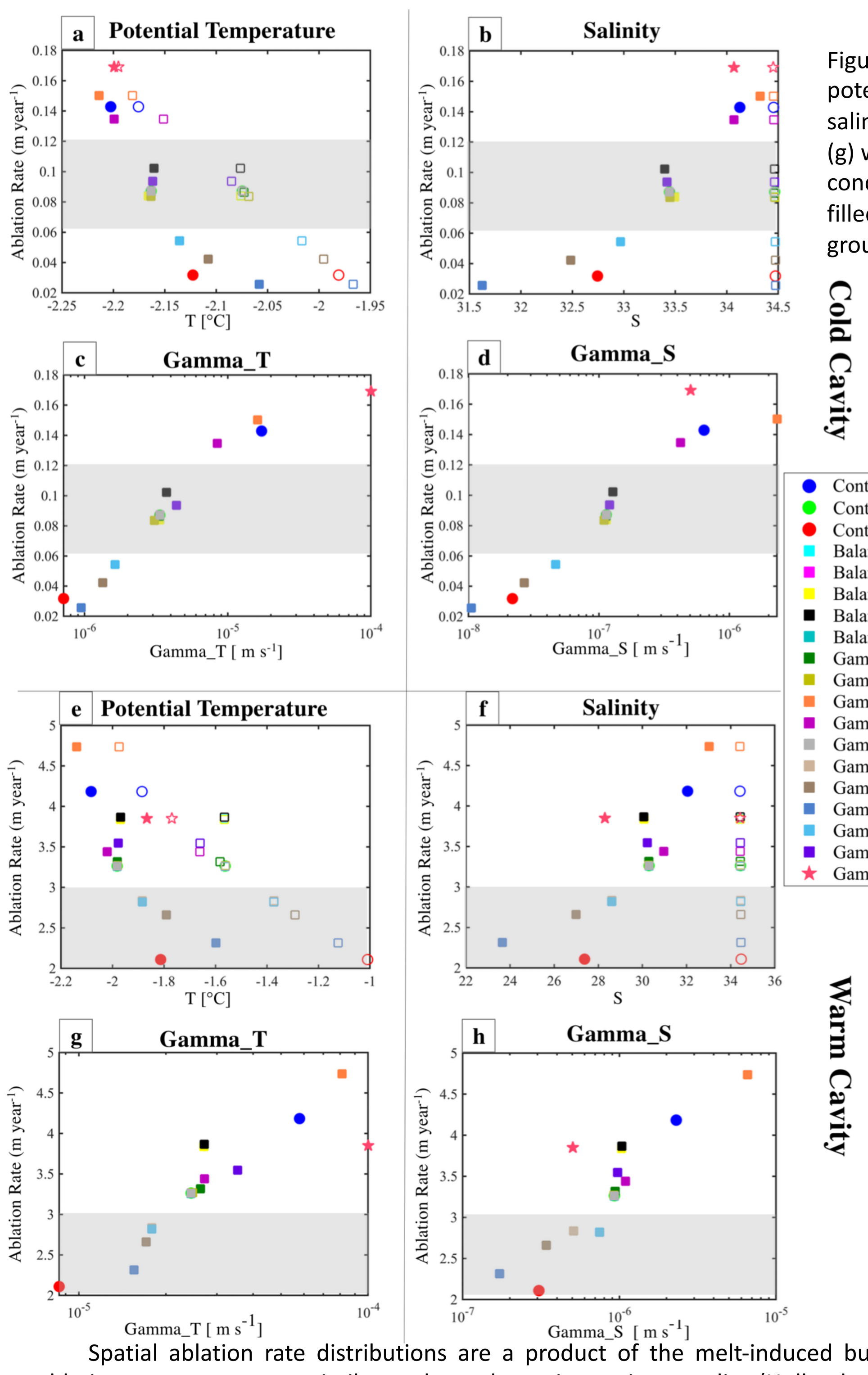

Figure 1. Summary values taken as spatial mean over the cavity: potential temperature in (a) cold and (e) warm cavity conditions; salinity in (b) cold and (f) warm cavity conditions; Γ_T in (c) cold and (g) warm cavity conditions; Γ_S in (d) cold and (h) warm cavity conditions. For temperature and salinity plots interface values are filled, and ocean values are unfilled. Grey shading indicates distinct groups associated with Γ_T values.

The range of values for Γ_T is 7.1×10^{-7} to 1.7×10^{-5} ms^{-1} in cold cavity conditions, and 8.5×10^{-6} to 8.1×10^{-5} ms^{-1} in warm cavity conditions (excluding constant value 10^{-4} m s^{-1} in Gamma_11). The cold cavity range includes observed Γ_T (0.0011×5 cm s^{-1}=5.5×10^{-5} ms^{-1}) from the Larsen C and Ronne Ice Shelf cavities under relatively smooth ice shelf bases (Davis and Nicholls, 2019; Jenkins et al., 2010). The warm cavity range is similar to tuned values of Γ_T from Nakayama et al. (2017), suggesting present day conditions in cavities in the Amundsen and Bellingshausen Seas are reflected in existing parameterisations.

Large ΔT and ΔS between the interface (filled markers in Fig. 1) and the center of the top cell (unfilled markers) can be interpreted differently. The interface values are defined as molecular sublayer values, and in that case large gradients can be realistic. Alternatively, ΔS~10 psu reflects lack of meltwater mixing in the top half cell of the ocean, that is not covered by the ocean mixing scheme and fully determined by $\Gamma_{T/S}$ values. In a model with only buoyancy-driven velocities, trapping meltwater in the top half cell leads to lower velocities.

Tidal velocities and C_d have only indirect effect on mixing through calculation of u_*, and those external velocity forces have to be sufficiently strong to override the "trapping" effect.

Spatial ablation rate distributions are a product of the melt-induced buoyancy force that drives the boundary layer flow. Simulated ablation rate patterns are similar to those shown in previous studies (Holland et al., 2008; Dansereau et al., 2014; Gwyther et al., 2015, 2016), despite being produced under a range of ablation parameterizations. Experiments in cold cavity conditions show three distinct patterns of spatial distribution of ablation and associated $\Gamma_{T/S}$ values (shown by the grey shading in Figure 2). An example of an experiment with high values of $\Gamma_{T/S}$ shows high ablation in the southeast corner and freezing along the western boundary (Gamma_3 in Figure 3a). Such examples resemble results with tidal dynamics from Gwyther et al. (2016). Experiments with medium values $\Gamma_{T/S}$ (e.g., Gamma_1 in Figure 3b) show a transitional ablation rate pattern with a small area of freezing in the northwest and highest ablation in the southwest. Experiments with lowest values of $\Gamma_{T/S}$ show enhanced ablation rates along the western boundary (e.g., Gamma_7 in Figure 3c).

Experiments with warm cavity conditions generate two patterns of ablation. Experiments with high and medium $\Gamma_{T/S}$ show high ablation along the eastern boundary, freezing in the northwest corner and lower ablation in the centre of the ice shelf (e.g., Gamma_3 & Gamma_1 in Figure 3d,e). As $\Gamma_{T/S}$ decreases, so does the ablation rate along the inflow in the east (e.g., Gamma_7 in Figure 3f). Exceptions are limited to Control_LD and Gamma_8 (Figure S3-S6), where ablation rates do not show significant easterly enhancement. Thus the ablation pattern in the velocity-dependent ablation parameterization is determined equally by $\Gamma_{T/S}$, C_d, and U_∞.

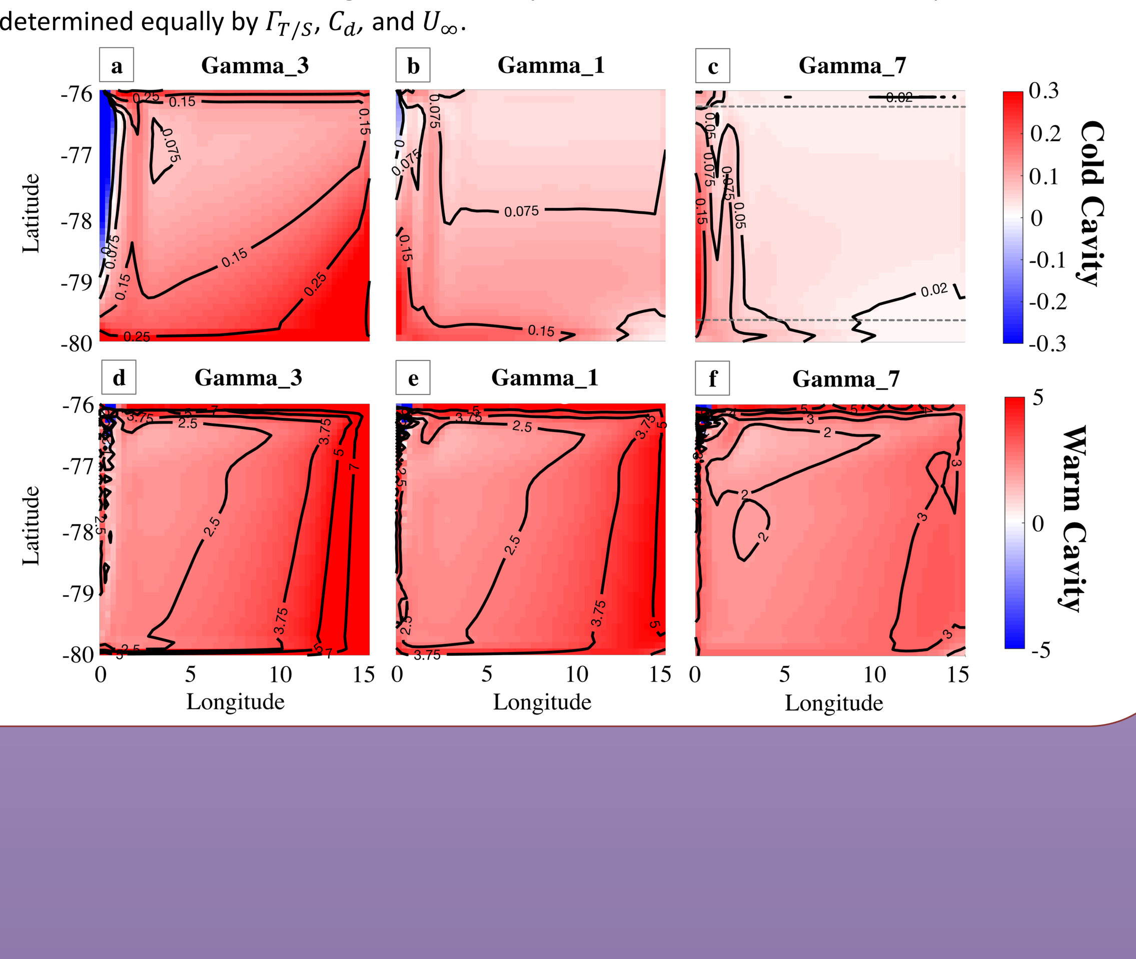

Figure 2. Maps of ablation rate for experiments in cold (top) and warm (bottom) cavity conditions: Gamma_3 (a, d); Gamma_1 (b, e); Gamma_7 (c, f). Note the change in color bar between cold and warm cavity experiments.

Vertical flux distribution

Three types of meltwater mixing were tested in order to move the meltwater away from the interface. The model domain stayed the same (ISOMIP domain 2). In case of ISOMIP forcing, the model run for 30 years, and the time-average of the last year is used in this analysis (same as in part 1 of the project, experiments are called warm and cold cavity). In case of ISOMIP+ forcing (Ocean0 and cold forcing; warm and cold cavity+) the model run for 5 years, and the time-average of the last year is used in this analysis (e.g., Gwyther et al., 2020). High ocean mixing case was tested with the same 12 experiments. In these tidal experiments, the northern boundary velocity is clamped to be 0.1 ms^{-1} with M2 period, and C_d =0.1.

The experiments are grouped as follows (Table 2):

- The first set is a repeat of Control experiment mixing: spreading of surface heat and salt fluxes into the top cell and further KPP mixing.
- The second set of experiments employs spreading the heat and salt flux evenly over top 20m of water column and further KPP mixing.
- The third set employs constant mixing coefficients for stable vs. unstable conditions and modifying tracer diffusion coefficients to create a well-mixed layer (following ISOMIP+ and ROMS modifications in Gwyther et al., 2020).

		KPP Mixing		KPP Mixing and Flux Spreading into 20 m		ISOMIP+ mixing and 20m mixed layer modification
Control Case No Tidal Forcing	ISOMIP	Control_KPP_c Control_KPP_w	ISOMIP	Control_Flux_c Control_Flux_w	ISOMIP	Control_ISOMIP_c Control_ISOMIP_w
	ISOMIP+	Control_KPP_c+ Control_KPP_w+	ISOMIP+	Control_Flux_c+ Control_Flux_w+	ISOMIP+	Control_ISOMIP_c+ Control_ISOMIP_w+
Gamma_3 + HD Tidal forcing	ISOMIP	Mixing_KPP_c Mixing_KPP_w	ISOMIP	Mixing_Flux_c Mixing_Flux_w	ISOMIP	Mixing_ISOMIP_c Mixing_ISOMIP_w
	ISOMIP+	Mixing_KPP_c+ Mixing_KPP_w+	ISOMIP+	Mixing_Flux_c+ Mixing_Flux_w+	ISOMIP+	Mixing_ISOMIP_c+ Mixing_ISOMIP_w+

Table 2. Experiments description and naming convention.

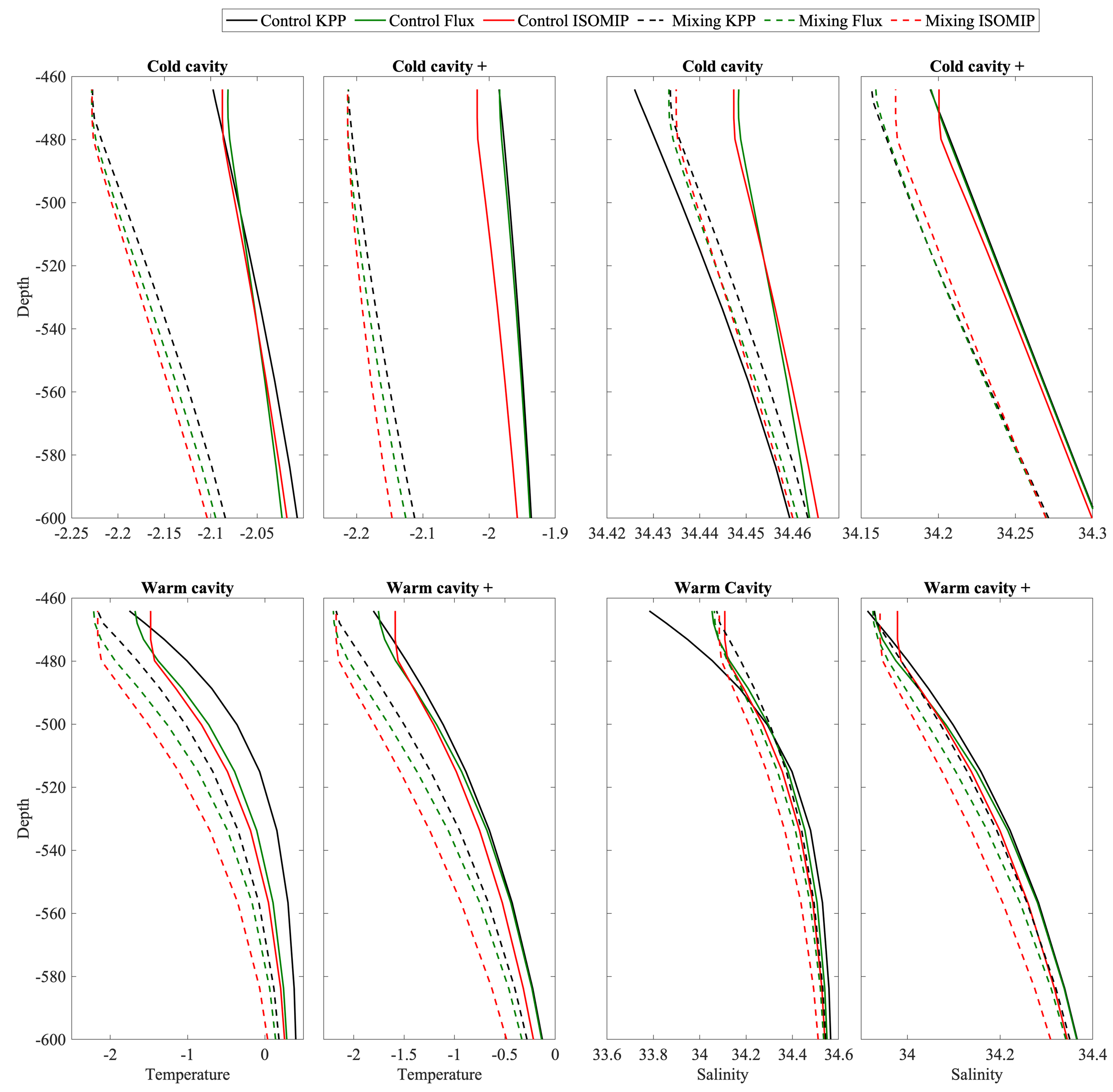

Figure 3. Profiles of temperature and salinity at the center of the cavity (melting location). All horizontal scales are different. The water column depth is 900m.

Both strategies of meltwater mixing are successful in creating a mixed layer next to the interface (Fig.3). ISOMIP+ mixing (red lines) creates sharper transition from the mixed layers to the ocean below then Flux Spreading due to large differences in stable and unstable coefficient values. Generally meltwater mixing leads to warmer and saltier values in the top ocean cell.

Ocean mixing experiments (dashed lines) show larger meltrates, thus colder and fresher profiles not just next to the interface, but in deeper layers too. Ocean mixing experiments do not produce a mixed layer next to the ice shelf base with KPP mixing, and do not make the mixed layer deeper in experiments with meltwater mixing (where the mixed layer already exists without tides). Possibly experiments with larger prescribed velocities and/or surface roughness will show a mixed layer formation.

Meltwater mixing and ablation rate

Figure 4. Summary values taken as spatial mean over the cavity: potential temperature and salinity. ISOMIP and ISOMIP+ forcing is plotted separately. Filled markers represent ocean mixing experiments.

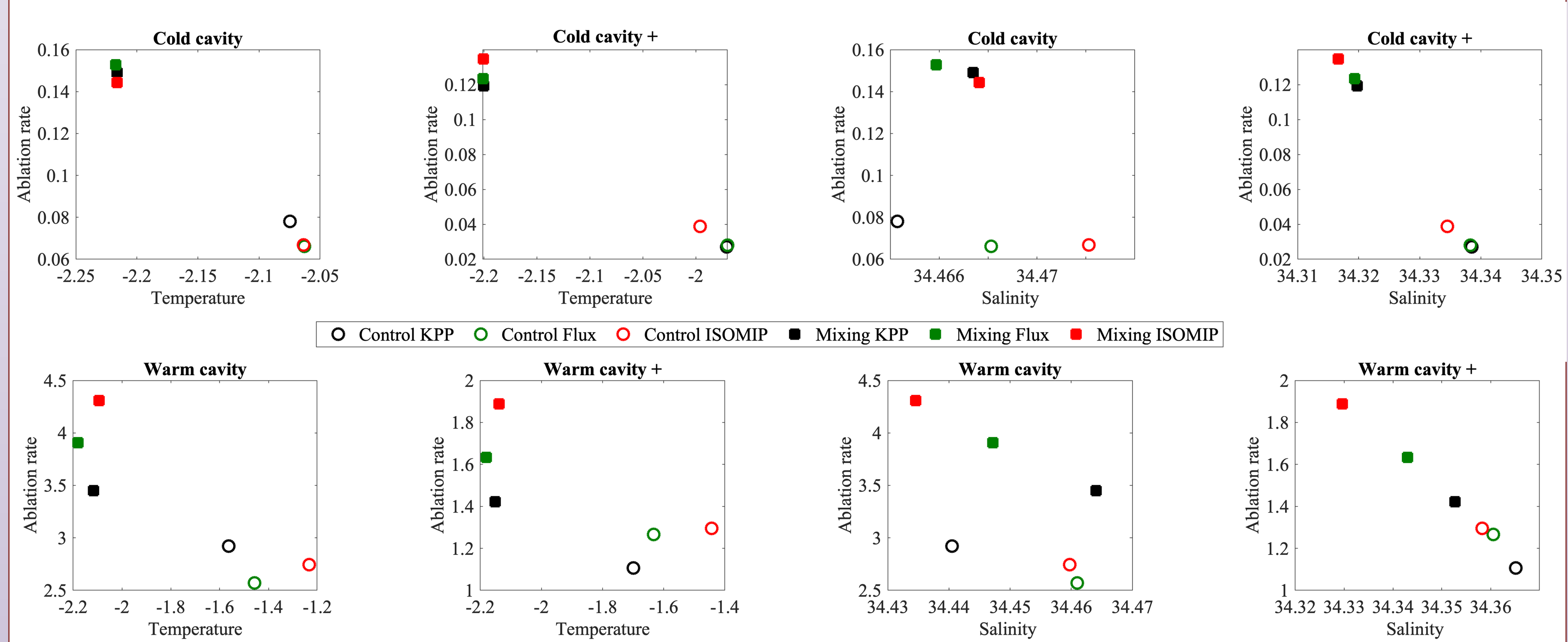

The initial and boundary conditions vary significantly between ISOMIP and ISOMIP+. In Part 1 of our project, the model is initialized with -1.9°C and 34.4 psu. Restoring the surface of ocean ocean does not immediately provide source of heat in the cavity. The warmer water eventually enters the cavity in the eastern part (right-hand side of plots in Fig.2), but there is a significant delay of signal closer to the grounding line. In contrast, initializing the water column with warmer waters already in the cavity, and providing 3-D restoring next to the northern boundary provides the ocean layers in most of the cavity with a source of heat right after the model initialization. Thus, meltwater mixing experiments showed different changes in the meltrate various initial conditions (circles in Figure 4). ISOMIP initial conditions lead to a decrease in meltrates when meltwater spreading is added: there is no warm water in the cavity. Lower initial meltrates lead to less developed buoyancy-driven circulation, further lowering the meltrates. Using ISOMIP+ initial condition, we saw the same effects as described in Gwyther et al. (2020): applying enhanced mixing in the boundary layer allowed ROMS model to be in contact with those warm waters and resulted in increased meltrates. Experiments with ISOMIP+ mixing used large values of vertical diffusivity and created more pronounced mixed layers (compare red and green lines in Figure 3), thus they also showed larger increase in meltrates. However, in ocean mixing experiments (filled squared in Figure 4) the results are not as clear. In cold cavities, meltwater mixing can both increase or decrease the meltrate. In warm cavities, the meltrate decreased for both ISOMIP and ISOMIP+ forcing. It is likely that the importance of buoyancy-driven circulation development decreases once the model has an external source of circulation. But the relative values of "tidal" and "buoyancy-driven" velocities need to be investigated further.

The "source of heat" is likely the cause of lower ablation rates in ISOMIP+ experiments compared to ISOMIP experiments. In ISOMIP+ experiments, the warmer ocean waters (+1°C) are positioned in lower part of the ocean, imitating inflow of CDW into the cavity. In ISOMIP experiments, warm water (+0.5°C) is located on the ocean surface and likely fills the cavity entirely by the end of the experiment. Exact pathways of heat over the whole model run need to be investigated to determine the feedbacks.

Ocean mixing experiments (Fig. 4, filled markers) expectedly showed larger meltrates, as we have used a velocity-dependent Gamma_3 parameterization. In all warm cavity experiments, meltwater mixing combined with ocean mixing lead to larger meltrates than Mixing_KPP (no meltwater spreading). In cold cavity experiments, the ablation rate values are much closer, and cold cavity experiment Mixing_ISOMIP_c showed reduction in the ablation rate compared to experiment with no meltwater spreading but Mixing_Flux_c showed increase in meltrate. While the meltwater mixing strategies have the same goal, some additional feedbacks associated with using the KPP mixing are likely to affect the result.

Conclusion and research priorities

Currently published ablation parameterisations have been largely based on calibration under sea ice. We have tested parameterisations in the idealised ice shelf-ocean model to assess the uncertainty range of these models. The models have a widespread in simulated ablation rates for all scenarios, both in value and in spatial distribution. Presently none of the parameterizations can be recommended for universal use and fitting modelled meltrate over a cavity to observations may provide the right numerical predictions in present day conditions but have little skill as ocean conditions change. Undertaking a standardised suite of observations of the ice-ocean boundary layer in a variety of ocean conditions would help to resolve the disparity between observation and simulation. For example, direct observations of characteristics and evolution under conditions with different ocean velocities and boundary roughness types in both warm and cold ocean cavities are recommended.

Further experiments of idealised ice shelf-ocean cavities may be beneficial to our understanding of the interplay between meltwater production and ocean mixing schemes. Our research plans include:

- Vertical resolution in the ice shelf cavity – how can we account for the volume of the ocean cell that receives the meltwater?
- Horizontal resolution in the ice shelf cavity – can tidal forcing interact with small-scale basal features?
- Maximum possible tidal forcing and very high boundary roughness – can they ever create a mixed layer?
- Tracer of warm water experiments – what is the path of heat into the cavity and how long does it take?
- Evolving ice shelf base experiments – are feedbacks significantly large ?